PHYSICAL REVIEW D **74,** 041502(R) (2006)

Quasiequilibrium sequences of black-hole–neutron-star binaries in general relativity

Keisuke Taniguchi,[1] Thomas W. Baumgarte,[2,*] Joshua A. Faber,[1] and Stuart L. Shapiro[1,†]
[1]*Department of Physics, University of Illinois at Urbana-Champaign, Urbana, Illinois 61801, USA*
[2]*Department of Physics and Astronomy, Bowdoin College, Brunswick, Maine 04011, USA*
(Received 19 May 2006; published 23 August 2006)

We construct quasiequilibrium sequences of black-hole–neutron-star binaries for arbitrary mass ratios by solving the constraint equations of general relativity in the conformal thin-sandwich decomposition. We model the neutron star as a stationary polytrope satisfying the relativistic equations of hydrodynamics and account for the black hole by imposing equilibrium boundary conditions on the surface of an excised sphere (the apparent horizon). In this paper we focus on irrotational configurations, meaning that both the neutron star and the black hole are approximately nonspinning in an inertial frame. We present results for a binary with polytropic index $n = 1$, mass ratio $M_{\rm irr}^{\rm BH}/M_{\rm B}^{\rm NS} = 5$, and neutron star compaction $M_{\rm ADM,0}^{\rm NS}/R_0 = 0.0879$, where $M_{\rm irr}^{\rm BH}$ is the irreducible mass of the black hole, $M_{\rm B}^{\rm NS}$ the neutron star baryon rest mass, and $M_{\rm ADM,0}^{\rm NS}$ and R_0 the neutron star Arnowitt-Deser-Misner mass and areal radius in isolation, respectively. Our models represent valid solutions to Einstein's constraint equations and may therefore be employed as initial data for dynamical simulations of black-hole–neutron-star binaries.

DOI: 10.1103/PhysRevD.74.041502 PACS numbers: 04.30.Db, 04.25.Dm, 04.40.Dg

Coalescing black-hole–neutron-star (hereafter BHNS) binaries are among the most promising sources of gravitational waves for laser interferometers [1–4]. BHNS mergers may reveal a wealth of astrophysical information (see e.g. [5]), and, along with mergers of binary neutron stars, are also considered primary candidates for central engines of short-duration gamma ray bursts (SGRBs) [6–8]. Recent observations of several SGRBs localized by the *Swift* and HETE-2 satellites in regions with low star formation strongly suggest that a compact binary merger scenario for SGRBs is favored over models involving the collapse of massive stars (see, e.g., [9] and references cited therein).

Significant effort has gone into the study of binary neutron stars and binary black holes, which are also promising sources of gravitational radiation. Fully relativistic simulations of BHNS binaries have received far less attention. Most BHNS calculations to date, including quasiequilibrium (QE) calculations [10–18] and dynamical treatments [19–25], employ Newtonian gravitation in either some or all aspects of their formulation. We have recently launched a new effort to study BHNS binaries in a fully relativistic framework (see also [26,27]), first by constructing QE models [28,29] and then by employing them as initial data in dynamical simulations [7,30]. So far we have focused on binaries for which the black hole mass is much greater than the neutron star mass. For binaries with such extreme mass ratios, the rotation axis can be taken to pass through the center of the black hole, and the tidal effects of the neutron star on the black hole may be ignored. These approximations simplify the problem considerably (see [28]). However, they break down for binaries containing comparable mass companions. Such systems are more suitable as SGRB candidates, because the tidal disruption of the neutron star by the black hole will occur near or outside the innermost stable circular orbit. This disruption may be necessary to create a gaseous accretion disk around the black hole capable of generating a SGRB [7]. Gravitational waves from BHNS binaries of comparable mass are detectable by ground based laser interferometers like LIGO (Laser Interferometric Gravitational-wave Observatory), while waves from systems with extreme mass ratios are much lower in frequency and require space-borne interferometers like LISA (Laser Interferometer Space Antenna).

In this paper we describe the construction of QE sequences of BHNS binaries with companions of comparable mass. We construct such binaries by solving the constraint equations of general relativity together with the relativistic equations of hydrodynamic equilibrium in a stationary spacetime assuming the presence of an approximate helical Killing vector (see, e.g., the recent reviews [31,32] as well as Sec. II of [33]). Throughout this paper we adopt geometric units with $G = c = 1$, where G denotes the gravitational constant and c the speed of light. Latin and Greek indices denote purely spatial and spacetime components, respectively.

The line element in 3 + 1 form can be written as

$$ds^2 = g_{\mu\nu}dx^\mu dx^\nu = -\alpha^2 dt^2 + \gamma_{ij}(dx^i + \beta^i dt)(dx^j + \beta^j dt), \quad (1)$$

where α is the lapse function, β^i the shift vector, γ_{ij} the spatial metric, and $g_{\mu\nu}$ the spacetime metric. Einstein's equations can then be split into constraint and evolution equations for the spatial metric γ_{ij}. To decompose the constraint equations we introduce a conformal rescaling

[*]Also at Department of Physics, University of Illinois at Urbana-Champaign, Urbana, IL 61801, USA
[†]Also at Department of Astronomy and NCSA, University of Illinois at Urbana-Champaign, Urbana, IL 61801, USA

$\gamma_{ij} = \psi^4 \tilde{\gamma}_{ij}$, where ψ is the conformal factor and $\tilde{\gamma}_{ij}$ the spatial background metric. The Hamiltonian constraint then reduces to

$$\tilde{\nabla}^2 \psi = -2\pi\psi^5\rho + \frac{1}{8}\psi\tilde{R} + \frac{1}{12}\psi^5 K^2 - \frac{1}{8}\psi^{-7}\tilde{A}_{ij}\tilde{A}^{ij}. \tag{2}$$

Here $\tilde{\nabla}_i$, $\tilde{R}_{ij}$, and $\tilde{R} = \tilde{\gamma}^{ij}\tilde{R}_{ij}$ denote the covariant derivative, the Ricci tensor, and the scalar curvature associated with $\tilde{\gamma}_{ij}$. We also decompose the extrinsic curvature K^{ij} into its trace (K) and traceless ($\tilde{A}^{ij}$) parts, $K^{ij} = \psi^{-10}\tilde{A}^{ij} + \gamma^{ij}K/3$.

In the conformal thin-sandwich decomposition we express the traceless part of the extrinsic curvature in terms of the time derivative of the background metric, $\tilde{u}_{ij} = \partial_t \tilde{\gamma}_{ij}$, and gradients of the shift. For the construction of equilibrium data it is reasonable to assume $\tilde{u}_{ij} = 0$ in a corotating coordinate system, which yields

$$\tilde{A}^{ij} = \frac{\psi^6}{2\alpha}\left(\tilde{\nabla}^i\beta^j + \tilde{\nabla}^j\beta^i - \frac{2}{3}\tilde{\gamma}^{ij}\tilde{\nabla}_k\beta^k\right). \tag{3}$$

Inserting this into the momentum constraint we then obtain

$$\tilde{\nabla}^2\beta^i + \frac{1}{3}\tilde{\nabla}^i(\tilde{\nabla}_j\beta^j) + \tilde{R}^i_j\beta^j = 16\pi\alpha\psi^4 j^i + 2\tilde{A}^{ij}\tilde{\nabla}_j(\alpha\psi^{-6}) + \frac{4}{3}\alpha\tilde{\gamma}^{ij}\tilde{\nabla}_j K. \tag{4}$$

It is also reasonable to assume $\partial_t K = 0$, which, from the evolution equation for the extrinsic curvature, yields

$$\tilde{\nabla}^2\alpha = 4\pi\alpha\psi^4(\rho + S) + \alpha\psi^{-8}\tilde{A}_{ij}\tilde{A}^{ij} - 2\tilde{\gamma}^{ij}\tilde{\nabla}_i\alpha\tilde{\nabla}_j\ln\psi + \frac{1}{3}\alpha\psi^4 K^2 + \psi^4\beta^i\tilde{\nabla}_i K. \tag{5}$$

Before we can solve the above set of gravitational field equations for ψ, β^i, and α, we still need to specify the spatial background metric $\tilde{\gamma}_{ij}$ and the trace of the extrinsic curvature K. We choose this background geometry to describe the Schwarzschild metric expressed in Kerr-Schild coordinates. Specifically, we choose $\tilde{\gamma}_{ij} = \eta_{ij} + 2M_{\rm BH}l_i l_j/r_{\rm BH}$ and $K = 2\hat{\alpha}^3_{\rm BH}M_{\rm BH}(1 + 3M_{\rm BH}/r_{\rm BH})/r^2_{\rm BH}$. Here η_{ij} is the flat spatial metric, $M_{\rm BH}$ is the "bare" mass of the black hole, $r_{\rm BH} = (X^2_{\rm BH} + Y^2_{\rm BH} + Z^2_{\rm BH})^{1/2}$ is the coordinate distance from the black hole center, $l_i = l^i \equiv X^i_{\rm BH}/r_{\rm BH}$ is the radial vector pointing away from the black hole center, and $\hat{\alpha}_{\rm BH} \equiv (1 + 2M_{\rm BH}/r_{\rm BH})^{-1/2}$ is the lapse function of the Schwarzschild metric in Kerr-Schild coordinates. The matter terms on the right-hand side of Eqs. (2), (4), and (5) are the projections $\rho \equiv n_\mu n_\nu T^{\mu\nu}$, $j^i \equiv -\gamma^i_\mu n_\nu T^{\mu\nu}$, $S_{ij} \equiv \gamma_{i\mu}\gamma_{j\nu}T^{\mu\nu}$, and $S \equiv \gamma^{ij}S_{ij}$ of the stress-energy tensor $T_{\mu\nu}$, where n_μ is the unit vector normal to the spatial hypersurface. Assuming an ideal fluid, we have $T_{\mu\nu} = (\rho_0 + \rho_i + P)u_\mu u_\nu + P g_{\mu\nu}$, where u_μ is the fluid 4-velocity, ρ_0 the baryon rest-mass density, ρ_i the internal energy density, and P the pressure.

The elliptic Eqs. (2), (4), and (5) require boundary conditions, both at spatial infinity and on the surface of an excised sphere within the black hole interior. At spatial infinity, where the metric becomes asymptotically flat in an inertial frame, we impose the exact boundary conditions, and on the excision surface (apparent horizon) we impose the black hole equilibrium boundary conditions suggested in [34]. To construct approximately nonspinning black holes we set the shift according to Eqs. (39) and (50) in [34] with $\Omega_r = \Omega_0$ in their notation. In the language of [35] this assignment corresponds to the "leading-order approximation," and we plan to improve this approximation as outlined there.

In addition to the field Eqs. (2), (4), and (5), we have to solve the equations of relativistic hydrodynamics. For stationary configuration, the relativistic Euler equation can be integrated once to yield

$$h\alpha\gamma/\gamma_0 = \text{constant}, \tag{6}$$

where $h = (\rho_0 + \rho_i + P)/\rho_0$ is the fluid specific enthalpy, and γ and γ_0 are Lorentz factors between the fluid, the rotating frame, and the inertial frame (see Sec. II.C. of [29] for the definitions). For irrotational fluids the fluid velocity can be expressed in terms of the gradient of a velocity potential Ψ. The equation of continuity then becomes

$$(\rho_0/h)\nabla^\mu\nabla_\mu\Psi + (\nabla^\mu\Psi)\nabla_\mu(\rho_0/h) = 0, \tag{7}$$

where ∇_μ is the covariant derivative associated with $g_{\mu\nu}$. We solve these equations for a polytropic equation of state $P = \kappa\rho_0^\Gamma$, where $\Gamma = 1 + 1/n$ denotes the adiabatic index, n is the polytropic index and κ is a constant. Here, we focus on the case $n = 1$ (i.e., $\Gamma = 2$).

We determine the orbital angular velocity by requiring that the derivative in the X direction of the enthalpy field at the center of the neutron star be zero, which implies that the total force balances at the center of the neutron star [29]. We confirm that the angular velocity obtained by this method agrees with that obtained by requiring the enthalpy at two points on the neutron star's surface be equal to within one part in 10^{-5} [28].

We locate the axis of rotation by requiring that the total linear momentum $P^i = \frac{1}{8\pi}\oint_\infty K^{ij}dS_j$ vanish [36]. To do so, we first align the axis of rotation with the Z axis and place the X axis to be the perpendicular line to the Z axis that passes through the black hole center. Given the equatorial symmetry in the problem, the Z component of the momentum vanishes automatically. With the orbital angular velocity held fixed, we drive the Y component of the linear momentum toward zero by adjusting the X coordinate of each companion, keeping their separation in the X direction unchanged. To determine their Y coordinates, we

require that the X component of the linear momentum be zero but only adjust the Y coordinate of the neutron star to achieve this. Thus, we fix the black hole's center to remain on the x axis at $Y = 0$.

Our numerical code uses the spectral method LORENE library routines developed by the Meudon relativity group [37]. The computational grid is divided into 10 (8) domains for a black hole (neutron star) and its exterior, and each domain is covered by $N_r \times N_\theta \times N_\phi = 33 \times 25 \times 24$ collocation points except for the closest two where 9 (8) domains are covered by $N_r \times N_\theta \times N_\phi = 25 \times 21 \times 20$ points.

In the following we focus on results for an inspiral sequence of constant irreducible black hole mass $M_{\rm irr}^{\rm BH}$ and neutron star baryon rest mass $M_{\rm B}^{\rm NS}$. In Table I we list results for a binary of mass ratio $M_{\rm irr}^{\rm BH}/M_{\rm B}^{\rm NS} = 5$ and a neutron star mass $\bar{M}_{\rm B}^{\rm NS} = 0.1$, where the bar denotes nondimensional polytropic units $\bar{M} = \kappa^{-n/2} M$. At infinite separation, this neutron star has a compaction $M_{\rm ADM,0}^{\rm NS}/R_0 = 0.0879$, where R_0 is the areal radius of the spherical star in isolation. In Fig. 1 we also show contours of the lapse α for the innermost configuration of this sequence. The value of the lapse everywhere on the black hole apparent horizon is set to be its Kerr-Schild value there, $2^{-1/2} = 0.7071$; its value at the center of the neutron star is 0.7275. Note that the center of the neutron star, as defined by the maximum of the enthalpy, does not coincide with the minimum point of the lapse inside the star. These configurations are the first fully relativistic QE models of BHNS binaries that do not assume an extreme mass ratio and employ equilibrium boundary conditions to model the black hole.

In the table we list the fractional binding energy $E_{\rm b}/M_0 \equiv M_{\rm ADM}/M_0 - 1$, total angular momentum J, orbital angular velocity Ω, maximum of the density parameter $q_{\rm max} = (P/\rho_0)_{\rm max}$, minimum of the mass-shedding indicator $\chi \equiv (\partial(\ln h)/\partial r)_{\rm eq}/(\partial(\ln h)/\partial r)_{\rm pole}$ [29,33], and fractional difference between the Arnowitt-Deser-Misner (ADM) mass and Komar mass $\delta M \equiv |1 - M_{\rm Kom}/M_{\rm ADM}|$. Quantities are tabulated as functions of the coordinate separation between the center of the black hole and the point of maximum baryon rest-mass density in the neutron star. Here, $M_0 = M_{\rm irr}^{\rm BH} + M_{\rm ADM,0}^{\rm NS}$ is the ADM mass of the binary system at infinite orbital separation, i.e., the sum of the irreducible mass of the isolated black hole and the ADM mass of an isolated neutron star with the same baryon rest mass. For an isolated Schwarzschild black hole, the ADM mass is the same as the irreducible mass.

TABLE I. Physical parameters for a binary sequence with mass ratio $M_{\rm irr}^{\rm BH}/M_{\rm B}^{\rm NS} = 5$ and neutron star compaction $M_{\rm ADM,0}^{\rm NS}/R_0 = 0.0879$ (where R_0 is the areal radius of the isolated neutron star). The baryon rest mass, the ADM mass, and the isotropic coordinate radius of the neutron star in isolation are $\bar{M}_{\rm B}^{\rm NS} = 0.1$, $\bar{M}_{\rm ADM,0}^{\rm NS} = 0.0956$, and $\bar{r}_0 = 0.990$ ($\kappa = 1$). We list the binding energy $E_{\rm b}$, total angular momentum J, orbital angular velocity Ω, maximum density parameter $q_{\rm max}$, mass-shedding indicator $\chi_{\rm min}$, and fractional difference δM between the ADM mass and the Komar mass.

d/M_0	$E_{\rm b}/M_0$	J/M_0^2	ΩM_0	$q_{\rm max}$	$\chi_{\rm min}$	δM
20.46	−7.18(−3)	0.679	1.10(−2)	5.83(−2)	0.892	7.95(−4)
18.41	−8.11(−3)	0.648	1.28(−2)	5.84(−2)	0.913	3.12(−3)
16.36	−9.22(−3)	0.615	1.52(−2)	5.86(−2)	0.953	6.41(−3)
14.32	−1.03(−2)	0.586	1.86(−2)	5.87(−2)	0.895	1.00(−2)
12.29	−1.13(−2)	0.556	2.36(−2)	5.75(−2)	0.843	1.43(−2)
10.26	−1.34(−2)	0.520	3.07(−2)	5.61(−2)	0.845	1.89(−2)
9.243	−1.47(−2)	0.502	3.59(−2)	5.56(−2)	0.791	2.07(−2)
8.741	−1.53(−2)	0.494	3.91(−2)	5.48(−2)	0.710	2.19(−2)
8.439	−1.58(−2)	0.488	4.11(−2)	5.42(−2)	0.588	2.27(−2)

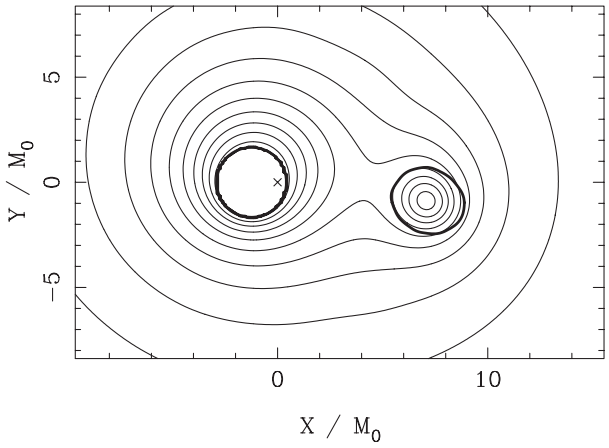

FIG. 1. Contours of the lapse α in the equatorial plane for the innermost configuration of the sequence listed in Table I. The thick circle on the left denotes the excision surface (apparent horizon) of the black hole, while that on the right denotes the surface of the neutron star. The cross "×" indicates the position of the rotation axis.

We compared our values for the angular momentum with those from third-order post-Newtonian approximations [38] and found agreement to within about 5% for close binaries, and better agreement for larger separations. In agreement with the third-order post-Newtonian results we do not see any indication of a turning point in the angular momentum, meaning that the tabulated sequence does not exhibit an innermost stable circular orbit, hence the binary orbits are all stable.

The quantity $\chi_{\rm min}$ is defined by the minimum of the indicator χ which compares the gradient of $\ln h$ at the pole with that on the equator. For spherical stars at infinite separation we have $\chi_{\rm min} = 1$, while $\chi_{\rm min} = 0$ indicates the formation of a cusp and hence tidal breakup. As we have discussed in [29], spectral methods no longer converge in the presence of discontinuities, so that our sequence terminates before reaching $\chi_{\rm min} = 0$. However, extrapolating from the last three data points we estimate that the star will be tidally disrupted when $\Omega M_0 \approx 0.046$. This value agrees with those estimated via the approximate

relativistic expansion of [18] ($\Omega M_0 \approx 0.043$) and the purely Newtonian models of [16] ($\Omega M_0 \approx 0.046$).

Equality between the ADM mass and Komar mass is equivalent to satisfying a relativistic virial theorem and indicates that the system is stationary (cf. [39]). In our calculation we do not impose this equality to construct the sequence, but instead evaluate mass difference as a diagnostic. For decreasing separation, the fractional difference between the two masses increases to over 2% for our innermost configuration. This clearly indicates that our closest models are not in perfect equilibrium. The resulting small, but finite, systematic mass difference has a large effect on the binding energy, which is also computed as the small difference between much larger masses.

We speculate that the differences between the ADM and Komar masses could be caused by our choice of the background geometry. Our choice of a Kerr-Schild background metric is motivated by our requirement that it correctly reduce to the exact solution for a spinning black hole in the limit of large separation (although here we only treat nonspinning holes). Also, in our coordinates, the lapse remains positive on the horizon (''horizon penetration''), which is necessary when computing $\tilde{A}_{ij}$ from Eq. (3). In [29] we compared with a flat background and found that the choice of the background has a small but nonvanishing effect on the physical properties of the resulting binary configurations (see also the discussion of nonmaximally sliced black hole binaries in [34]), motivating our speculation that our choice here may result in the small but systematic deviation from perfect equilibrium. Our configurations are solutions to the constraint equations and are hence adequate initial data for dynamical simulations of BHNS binaries (our main motivation here). We are currently experimenting with other background solutions to find better approximations to quasiequilibrium. However, this discrepancy in mass also heightens interest in the recent ''waveless'' formulation of the initial value problem that is based on the equality of the ADM and Komar masses and avoids the need to choose a background geometry altogether [40,41].

Finally, we turn our attention to the validity of QE configurations in circular orbit as initial data for dynamical simulations. The assumption of circular orbits and an associated helical Killing vector for relativistic binaries is an approximation, since the emission of gravitational waves leads to orbital decay. This approximation breaks down at a certain binary separation when the inspiral can no longer be ignored. We can quantify the departure from true QE by comparing the time scale of the orbital period with that of the orbital decay driven by the emission of gravitational waves. To lowest order we can estimating the ratio between these two time scales with the help of the quadrupole formula for Newtonian point masses, which yields

$$\frac{t_{\rm orb}}{t_{\rm GW}} \simeq 0.21\left(\frac{d_{\rm min}}{d}\right)^{5/2}\left(\frac{\nu}{0.135}\right). \tag{8}$$

Here $\nu \equiv M^{\rm BH}M^{\rm NS}/(M^{\rm BH}+M^{\rm NS})^2$ and $d_{\rm min}$ denotes the closest binary separation we computed in this paper (the value of the last line in Table I). It is reasonable to approximate the binary orbit as circular as long as the ratio $t_{\rm orb}/t_{\rm GW}$ is significantly smaller than unity (compare the discussion in [42]). For $d = d_{\rm min}$, we have $t_{\rm orb} \approx 0.2 t_{\rm GW}$, and for larger separations the ratio $t_{\rm orb}/t_{\rm GW}$ falls off with $d^{-5/2}$. For these separations it is therefore reasonable to neglect the inspiral and construct binaries in circular orbits and in the presence of a helical Killing vector.

In summary, we compute sequences of BHNS binaries with comparable mass companions. We solve the constraint equations of general relativity in the conformal thin-sandwich decomposition, subject to equilibrium black hole boundary conditions, together with the relativistic equations for hydrodynamic equilibrium in a stationary spacetime. We construct irrotational binaries, adopt a polytropic equation of state for the neutron star, and choose the background geometry to be a Schwarzschild black hole expressed in Kerr-Schild coordinates. As an example, we present results for a binary of mass ratio $M^{\rm BH}_{\rm irr}/M^{\rm NS}_{\rm B} = 5$ and neutron star of compaction $M^{\rm NS}_{\rm ADM,0}/R_0 = 0.0879$. To the best of our knowledge, these are the first models of quasiequilibrium, circular orbit, relativistic BHNS binaries with companions of comparable mass.

J. A. F. is supported by NSF Grant No. AST-0401533. This paper was supported in part by NSF Grants No. PHY-0205155 and No. PHY-0345151, and NASA Grant No. NNG04GK54G, to University of Illinois at Urbana-Champaign, and NSF Grant No. PHY-0456917 to Bowdoin College.

[1] G. González (LIGO Scientific Collaboration), Classical Quantum Gravity **21**, S691 (2004).
[2] M. Hewitson, P. Aufmuth, C. Aulbert, S. Babak, and R. Balasubramanian, Classical Quantum Gravity **20**, S581 (2003).
[3] M. Ando (TAMA Collaboration), Classical Quantum Gravity **19**, 1409 (2002).
[4] F. Acernese (VIRGO Collaboration), Classical Quantum Gravity **21**, S709 (2004).
[5] M. Vallisneri, Phys. Rev. Lett. **84**, 3519 (2000).

[6] M. Shibata and K. Taniguchi, Phys. Rev. D **73**, 064027 (2006).
[7] J. A. Faber, T. W. Baumgarte, S. L. Shapiro, and K. Taniguchi, Astrophys. J. **641**, L93 (2006).
[8] D. J. Price and S. Rosswog, astro-ph/0603845.
[9] E. Berger, in *Proceedings of the 16th Annual Astrophysics Conference on Gamma Ray Bursts in the Swift Era, Maryland*, edited by S. Holt, N. Gehrels, and J. Nousek, astro-ph/0602004..
[10] S. Chandrasekhar, *Ellipsoidal Figures of Equilibrium* (Yale University Press, New Heaven, CT, 1969).
[11] L. G. Fishbone, Astrophys. J. **185**, 43 (1973).
[12] D. Lai, F. A. Rasio, and S. L. Shapiro, Astrophys. J. Suppl. Ser. **88**, 205 (1993).
[13] D. Lai and A. G. Wiseman, Phys. Rev. D **54**, 3958 (1996).
[14] K. Taniguchi and T. Nakamura, Prog. Theor. Phys. **96**, 693 (1996).
[15] M. Shibata, Prog. Theor. Phys. **96**, 917 (1996).
[16] K. Uryū and Y. Eriguchi, Mon. Not. R. Astron. Soc. **303**, 329 (1999).
[17] P. Wiggins and D. Lai, Astrophys. J. **532**, 530 (2000).
[18] M. Ishii, M. Shibata, and Y. Mino, Phys. Rev. D **71**, 044017 (2005).
[19] B. Mashhoon, Astrophys. J. **197**, 705 (1975).
[20] B. Carter and J.-P. Luminet, Astron. Astrophys. **121**, 97 (1983); Mon. Not. R. Astron. Soc. **212**, 23 (1985).
[21] J.-A. Marck, Proc. R. Soc. London A **385**, 431 (1983).
[22] W. H. Lee and W. Kluźniak, Astrophys. J. **526**, 178 (1999); Mon. Not. R. Astron. Soc. **308**, 780 (1999).
[23] W. H. Lee, Mon. Not. R. Astron. Soc. **318**, 606 (2000); **328**, 583 (2001).
[24] S. Rosswog, R. Speith, and G. A. Wynn, Mon. Not. R. Astron. Soc. **351**, 1121 (2004).
[25] S. Kobayashi, P. Laguna, E. S. Phinney, and P. Mészáros, Astrophys. J. **615**, 855 (2004).
[26] M. Miller, gr-qc/0106017.
[27] C. F. Sopuerta, U. Sperhake, and P. Laguna, gr-qc/0605018.
[28] T. W. Baumgarte, M. L. Skoge, and S. L. Shapiro, Phys. Rev. D **70**, 064040 (2004).
[29] K. Taniguchi, T. W. Baumgarte, J. A. Faber, and S. L. Shapiro, Phys. Rev. D **72**, 044008 (2005).
[30] J. A. Faber, T. W. Baumgarte, S. L. Shapiro, K. Taniguchi, and F. A. Rasio, Phys. Rev. D **73**, 024012 (2006).
[31] G. B. Cook, Living Rev. Relativity **3**, 5 (2000).
[32] T. W. Baumgarte and S. L. Shapiro, Phys. Rep. **376**, 41 (2003).
[33] E. Gourgoulhon, P. Grandclément, K. Taniguchi, J.-A. Marck, and S. Bonazzola, Phys. Rev. D **63**, 064029 (2001).
[34] G. B. Cook and H. P. Pfeiffer, Phys. Rev. D **70**, 104016 (2004).
[35] M. Caudill, G. B. Cook, J. D. Grigsby, and H. P. Pfeiffer, gr-qc/0605053.
[36] J. M. Bowen and J. W. York, Jr., Phys. Rev. D **21**, 2047 (1980).
[37] LORENE web page, http://www.lorene.obspm.fr/.
[38] L. Blanchet, Phys. Rev. D **65**, 124009 (2002).
[39] E. Gourgoulhon, P. Grandclément, and S. Bonazzola, Phys. Rev. D **65**, 044020 (2002).
[40] M. Shibata, K. Uryū, and J. L. Friedman, Phys. Rev. D **70**, 044044 (2004).
[41] K. Uryū, F. Limousin, J. L. Friedman, E. Gourgoulhon, and M. Shibata, gr-qc/0511136.
[42] M. D. Duez, T. W. Baumgarte, S. L. Shapiro, M. Shibata, and K. Uryū, Phys. Rev. D **65**, 024016 (2002).